Modeling and Mitigation of dv/dt and Transmission Line Effect for Motor Drive System in Electric Aircraft Propulsion

Bo Liu
RTX Research Center (RTRC)
RTX
East Hartford, CT, USA
bo.liu@rtx.com

Xin Wu
Pratt & Whitney
RTX
East Hartford, CT, USA
xinwuxw@gmail.com

Alex Leary
Materials and Structures Division
NASA Glenn Research Center
Cleveland, OH 44135, USA
alex.m.leary@nasa.gov

Kushan Choksi
Department of Electrical and Computer Engineering
Stony Brook University
Stony Brook, USA
hoksi.kushan@stonybrook.edu

Yuxuan Wu
Department of Electrical and Computer Engineering
Stony Brook University
Stony Brook, USA
yuxuan.wu@stonybrook.edu

Fang Luo
Department of Electrical and Computer Engineering
Stony Brook University
Stony Brook, USA
fang.luo@stonybrook.edu

***Abstract*—Due to constraints in space and structure as well as other practical limitations in aircraft system, the motor controller or electric motor are often installed far away from each other and interconnected via long cables. This amplifies the transmission line effect excited by the dv/dt PWM voltage and induces high voltage stress on the machine winding. This paper investigates the state-of-art modeling approaches for such systems, identifies several limitations in matching the tested voltage reflection waveform in terms of peak voltage, oscillation frequency and damping speed, and offers several key considerations not well covered in literature or in engineering practice. It then proposes a practical modeling methodology which, as validated by experimental results, truly captures these critical reflection voltage specs. To mitigate the high peak voltage and strong oscillation, *dv/dt* filter is applied and a parametric design optimization based on widely adopted LC-R topology is illustrated, which not only alleviates the voltage stress but also minimized the power loss of the passive damping resistor.**

Keywords—dv/dt filter, SiC, Motor Drive, Transmission line, Electrified Propulsion

I. INTRODUCTION

In recent years, electric propulsion and hybrid propulsion are deeply investigated across various design aspects by industries and academia. Owing to functional and safety requirements as well as space constrains of aircraft, the motor controller and the electric motor may be placed far from each other, requiring cables with lengths of tens of or hundreds of feet for interconnection. The high voltage spike induced by the dv/dt transient of the motor controller becomes a concern, as the transient produced in the controller can be amplified several times higher by the cable transmission line effect at the motor winding terminals and potentially damage or threaten the insulation and lifetime of the motor [1]. The effects of the imposed voltage spike are most pronounced within the first several turns of motor windings or the turns near to the three-phase neutral connection [12]. This issue has become more severe with the emerging of wideband gap (WBG) technologies and high voltage SiC devices gradually adopted in high power motor driving applications, since the dv/dt of SiC devices is ten times higher than its counterpart IGBT [2] and even a much shorter cable system will likely suffer the similar voltage peaks. Moreover, the transmission line effect also induces high frequency (HF) ringing on the cables, amplifying both conducted and radiative EMI noises. It is also recently reported a low frequency common-mode (CM) voltage oscillation at the machine antiresonant frequency could be incurred inside the stator windings across the coils close to the neutral [12]. Induced excessive voltages due to the high dv/dt excitation can also exist regardless of the cable length [12], further necessitating the need to tackle these challenges. These voltage transients related to interconnection impedances between and within system components could also occur in turboelectric propulsion systems where the generator and active rectifier interact in the similar way.

To mitigate the dv/dt effects, the dv/dt filter is the key element to slow down the dv/dt of the inverters and must be developed for aviation power systems. Given the noticeable power loss in the filter, a design optimization is desired to not only achieve the target reflection voltage suppression but also ensure low power loss including both the resistance loss from the damping resistor and inductor winding as well as the magnetic core loss.

Therefore, proper high frequency modeling approaches with high fidelity for such drivetrains as well as a sound and efficient design methodologies of the passive filter become crucial. This paper leverages and discusses the historical and state-of-art modeling work on power cable and transmission line

This work was funded by the NASA Advanced Air Transport Technology Project, Power and Propulsion Subproject.

in motor driving systems [1, 4, 12-14, 16-18], and presents a practical and simple approach to model the system and design the dv/dt filter. It also highlights several additional factors that should be considered such as additional interfacing cable between the motor controller and dv/dt filter to ensure high fidelity modeling. A design example will be presented, and experimental results provided that show the accuracy of the model with and without the filter.

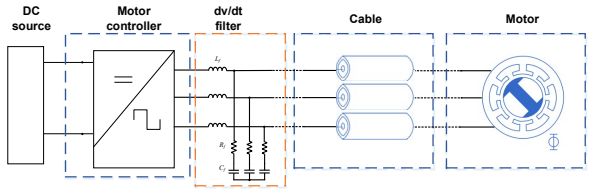


Fig. 1. A typical motor drive system with a dv/dt filter to mitigate reflection voltage spike and ringing.

II. Modeling of Transmission Line Overvoltage

This section overviews the state-of-art modeling approaches for ac cables, power converters, and motors, and provides several additional observations and insights for modeling such systems in practical test implementation.

A. Cable Modeling

1) Lumped models

The reflection voltage for a given excitation on a transmission line is related to the phase velocity $v = 1/\sqrt{\mu\epsilon}$ where μ and ε are the permeability and permittivity of the line. The key in modeling of ac power cables is to capture their high frequency behaviors since reflection voltage ringing frequency within the cable could be several MHz depending on the system scale, whose first reflection point occurs at $v/4l$ and l is the cable length. The lumped parameter model formed by per meter (per unit) inductance-capacitance-conductance-resistance (LCGR) parameters is the simplest way for modeling the transmission line. However, a single Π or Γ section is typically insufficient to reflect energy at the high frequency of interest. In cables, the permeability is usually small so an approximated maximum frequency represented by Π or Γ model can be determined by

$$f_{max} = N \cdot \frac{v}{8l} = N \cdot \frac{c}{8l\sqrt{\varepsilon_r}}, \quad (1)$$

where N is the number of cascaded PI sections, v is the wave speed mainly affected by relative permittivity ε_r of the cable medium [15]. On the other hand, the maximum frequency from the power converter output can be set at the first cutoff point of its voltage spectrum with a margin factor k if needed [12-14],

$$f_{max} = k \cdot 1/\pi \cdot min(t_r, t_f), \quad (2)$$

where k is the margin factor, default at 1, and t_r, t_f are the rising and falling time of output voltage edges, respectively.

From Equations (1) and (2), one can decide the section number N. Alternatively, N could also be selected smaller enough than the wavelength at f_{max}.

The skin and proximity effects: the cable impedance is strongly frequency dependent. Several methods have been proposed for higher accuracy in time domain simulation. Ladder circuit models with fixed parameters give high accuracy, but at the expense of resolving multiple R-L circuit parameters in the ladder network [12,14,19]. A simplified first-order R-L parallel branch has also been used when only considering a relatively low frequency range of interest. A further delta R plus first-order R-L method is also proposed which provides the exact resistance at the interested oscillation frequency reference to the measured value with lower complexity but allows certain errors at other frequencies [14]. The cable inductance is also a function of frequency which could also be modeled in further efforts, however since the change is typically small, the impact could be neglected.

2) Distributed models

Distributed transmission line models can also be considered for more accurate cable modeling at the expense of higher computation loading and implementation efforts. Several commercial circuit simulation software also provides such models like LTspice and Simulink. To further speed up the simulation, Bergeron models based on moment of methods are often used, particularly in power system EMTP software [17]. However, to include the frequency-dependent parameters, all these models need to be expanded: 1) a simple approach is again to only provide the exact AC resistance at the target frequency for specific study [16]; 2) or traditionally, to use inverse transforms and convolutions which results in more computation efforts and several restrictions in simulations of time-variable power components and non-linear phenomena [17]; 3) to apply the fitting method well adopted in lumped line models which emulates the longitudinal impedance as a rational function of the R-L network; 4) To represent more accurately the distributed characteristic of the line electrical parameters and model the very long transmission with wide frequency dynamics and fast transients, a cascade of modified Bergeron's circuits was also proposed [17].

3) Obtaining the per unit line parameters

Measurement: the per unit parameters used in the above models are typically obtained from cable impedance measurement using short-circuit and open-circuit approaches [16]. Due to the frequency-dependent characteristics of the impedance, schemes on how to derive these key line parameters with the frequency of interests (from low frequency to high frequency end) are reported [20] and illustrated in Fig. 2. One of the tricks is to decouple the self and coupling inductance in multiple phase cables, and another practical challenging is to properly measure the frequency-dependent cable ac resistance with high accuracy through several or tens of MHz range.

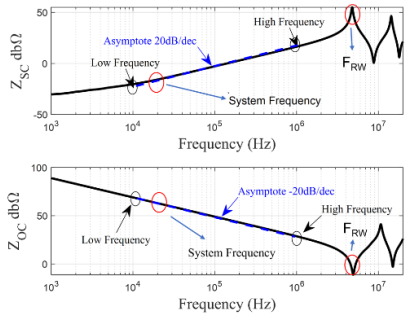


Fig. 2: Line parameter extraction based on impedance measurements of short circuit & open circuit and HF & LF range selection.

Analytical modeling or FEM simulation: analytical models based on transmission line theory and electromagnetic field analysis have been developed for various cables configuration with single or multiple conductors [18-19].

Remarks on inductance modeling: Analytical models for the inductance calculation of the unshielded line-line cables or single coaxial cable (shield as return path) is accurate. However, when considering strongly shielded line-line cables (one forward and one return, each has its own shield), such models seem only accurate at relatively low frequency but degrade at higher frequency based on the testing. The state-of-art model has not considered the impact of the shield of single-wire cable yet. From our observation, the negative coupling and skin effect seems stronger at the high frequency range due to the shield layer. More research might be needed in this area.

Remarks on resistance modeling: For resistance modeling, a good match has been observed with measurements below hundreds of kHz for the shielded cables. However, above this frequency range, analytical results show significantly underestimated values based on our preliminary study. This will highly impact the accuracy of reflection voltage modeling since the strong damping effect might be underestimated using the calculated low ac resistance at MHz range. It is also noted that mixed accuracy performance has been reported in literature for the analytical model [21-22]. Similar to the inductance modeling, further research is needed here.

B. Power Converter Modeling

For dv/dt filter design, the power converter is traditionally simplified as an ideal PWM step source or source with predefined dv/dt slope [23]. This approach is simple but does not truly represent the actual excitation source of the PWM converters. It is also unable to capture the accumulated impact of adjacent pulses on reflection voltage amplification [1]. More importantly, it fails to present the interaction between the source and the cable when reflection voltage is traveling back and forth due to the impedance mismatch in the interconnected driving system.

A simpler approach using measured open-loop terminal voltages of PWM converters could also simplify the excitation source modeling by offering the actual source voltage patterns, however, it fails for the same reason on impedance interaction. Details can be found in Fig. 6.

Therefore, to provide a high fidelity model that includes the reflection voltage, a detailed converter model including parasitic inductances and parasitic grounding capacitances is recommended. When switching speed and the converter output dv/dt matches the actual condition, this method can predict the results with good accuracy. The switching speed affects the overshoot significantly and the parasitics inside the converter also affect the overshoot, while the ringing frequency on the cable is determined by the passive cable impedances.

Further, we have found that when a short length interface wire is used to bridge the PWM converter and main ac cable due to various geometric constraints on direct connection in a test environment, a surprisingly high mismatch could be introduced between modeling and test result if the impedance of this short interface cable is neglected in the model, as shown in Fig. 3. This could be improved as later shown in Section D.

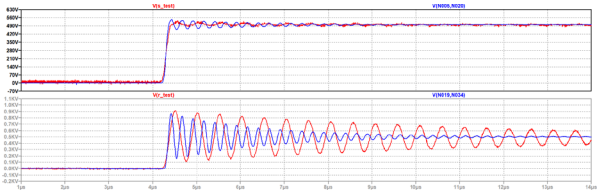


Fig. 3. Reflection voltage of modeling (in blue) and testing (in red) results without including the interface wire's impedance in the model. Top: converter. Bottom: cable far-end side.

C. Motor Modeling

For reflection voltage or EMI study, typical motor modeling approaches are based on a single cell lumped transmission line model consisting of phase inductance and resistance, turn-turn winding capacitance, and shaft leakage capacitance as well as the chassis grounding capacitance, either based on geometric derived analytical model or common-mode and differential-mode impedance measurement. However, this type of model is not suitable for overvoltage stress and oscillation study inside motor windings. The more comprehensive model with cascaded lumped cells considering turn-to-core, turn-to-turn capacitance, and turn inductance and resistance and their mutual couplings as well as R-L ladder based frequency-dependence in each cell can be found in [12-13], providing high accuracy.

D. Proposed Overall System Modeling

Based on the discussions, a practical modeling approach and verification test rig is proposed for the reflection voltage estimation and dv/dt filter design. As shown in Fig. 3, on the converter side, the three-phase motor drive is reconfigured to be a half bridge tester and used as the excitation source that can output double pulses or continuous pulses to study how the pulse gaps or modulation index impacts the reflection voltage. On the cable end, three-phase shielded cables are formed as a single loop whose two phases out of three are connected and paralleled to form the return path. On the load end, considering the generic usage of a motor drive and dv/dt filter for potentially different motors or loads, the no load condition is adopted. Although the motor impedance may have certain impacts on the motor terminal stress, open circuit creates the worst scenario with the highest voltage stress due to full voltage reflection [1], and verification of cable model accuracy and attenuation performance of dv/dt filter also does not need the motor. Hence an open circuit simulation/test with cables would be sufficient for the purpose here. This also avoids the unnecessary complexity for motor modeling. If the focus is on motor's internal winding voltage distribution and turn-turn insulation stress, a detailed motor model is certainly required.

The switches of the pulse tester are modeled with spice models from the power device vendors. The circuit parasitics are also included in the circuit model, which can be extracted either from Ansys Q3D analysis typically performed at the design stage of the motor drives, the component datasheets, or measurements from double pulse testing. The main cables are modeled with multiple cascaded lumped Γ sections of parameters measured via the method in section II. B where frequency dependent ac resistance is also considered.

Due to the limitation of the test rig, a several feet long interfacing wire) is adopted between the converter terminals and bulky three-phase motor cables. As discussed before, its inductance and resistance (Ls1-Rs1 in Fig. 4) shall also be included in the model. The shorter or bigger the cable is, the lower its impact on reflection voltage stress is. An effort has been made to minimize this set of wire as short as possible in the setup.

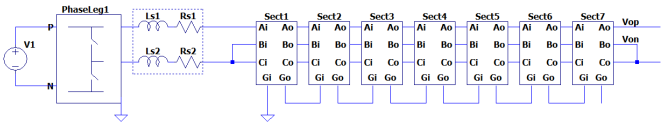


Fig. 4. LTspice based simulation model with a phase leg of PWM converter (masked) and 7 sections of 1-meter lumped Γ shape cable model.

The detailed cable impedance model of the three-phase is provided in Fig. 5 for one section, where the paralleled R-L represents the skin/proximity effect related ac resistance. The couplings among the line inductances are also included.

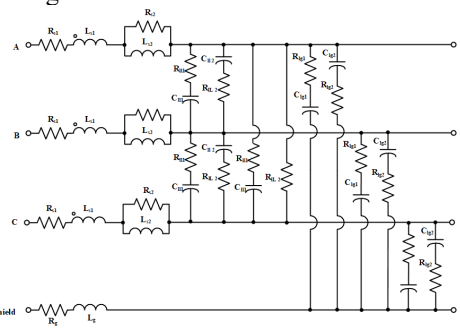


Fig. 5. Cable impedance model per section for the three-phase shielded cables.

As discussed before, any potential interface wire between cable and inverter should be considered in the simulation model. Fig. 6 illustrate the significant difference when the 0.48 μH inductance of a short interface wire is considered, compared to poor modeling accuracy in Fig. 3.

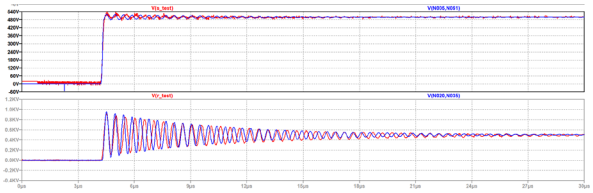


Fig. 6. Reflection voltage of modeling (in blue) and testing (in red) results (bottom) when including the impedance of the interface wire in the model. Top: converter side. Bottom: cable far-end side.

A comparison is also conducted between the presented modeling approach and a simplified method one may attempt. As illustrated in Fig. 7, the simplified method incorporates the measured PWM voltage waveforms of the converter terminals as an ideal voltage excitation source to the cable impedance.

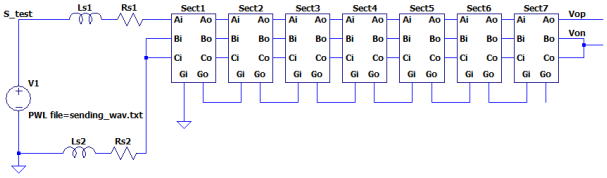


Fig. 7. LTspice based simulation model using measured PWM converter waveform as ideal excitation source.

It is clearly seen from Fig. 8, the simplified method shows quite different peak voltage and oscillation damping pace. It might be acceptable to predict the first peak of load side voltage but fails to predict correctly the whole behaviors after that. This is likely due to the break of the interaction of traveling wave reflection when the converter side is brutely modeled by a controlled voltage source.

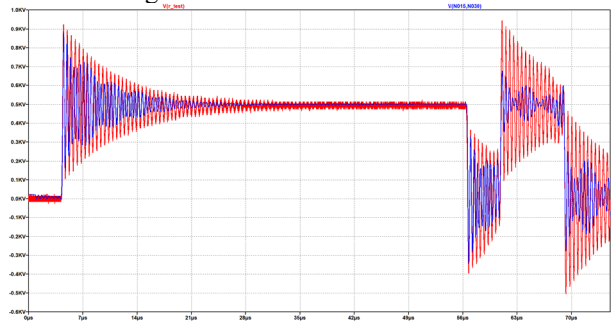


Fig. 8. Reflection voltage of modeling (in blue) and testing (in red) results based on the simplified modeling approach with measured PWM output voltage waveforms as the excitation source to eliminate converter modeling.

III. DV/DT FILTER DESIGN

The motor terminal voltage spike can be potentially higher above 2 p.u. if the voltage ringing is not fully attenuated before the onset of another voltage pulse within a pulse gap period of 3τ (time constant) [1]. With very short pulse gaps, the overvoltage could be higher than 3 p.u. depending on the cable length and per unit L and C. Although elimination of short pulses in motor controller is possible through the digital control [1], the effect on power quality might be a concern. Impedance matching theory provides a more acceptable approach to tackle dv/dt spikes. A common practice in very high power motors with IGBT drives places a RC terminator in parallel to motor phase terminal. On the source side, sine filter or dv/dt filters are common, especially for lower and medium power drives, where dv/dt filter is more attractive for high-speed high-density SiC based drives with the sole purpose to smooth the high dv/dt edge and sine filter is a better choice for extremely long cables and a strong voltage suppression need.

A. Parameter Selection

The common LC-R dv/dt filter as shown in Fig. 1 is adopted in this design, where the damping R is in series with the C branch. To achieve decent filter performance and minimal damping loss, an optimized design is proposed through the parametric analysis of LCR values considering multi-targets: peak voltage stress, filter loss, and damping resistor pulse power. Thanks to the high-performance magnetics applied in the design, the inductor loss is small compared to the damping resistor. With properly selected chassis mount power resistor such as TAP800 series from Ohmite, the pulse power rating within 10 μs is high up to 1000 kW, sufficient for most of the design conditions. Those help narrow the targets to cable far-end voltage stress and damping resistor loss.

As illustrated in Fig. 9, higher series inductance helps reduce the peak overvoltage at the cable far-end side, while its impact on the R loss is dependent on the RC combinations. On the other hand, higher capacitance helps reduces the overvoltage but results in higher I^2*R loss. The impact of R on its power loss

is dual-fold, since higher R reduces the current within a certain degree but may still contribute to I^2*R loss. As expected, the peak voltage is the lowest in the medium range of R variation, around the cable characteristic impedance. Considering these factors, a brute force based 3-D parameter sweep is developed for the simulation model which automatically collects the voltage and current waveforms and captures the peak voltage and average loss over the switching cycle. At the end of these simulation, the lowest power loss design providing the target peak voltage reduction can be finally selected.

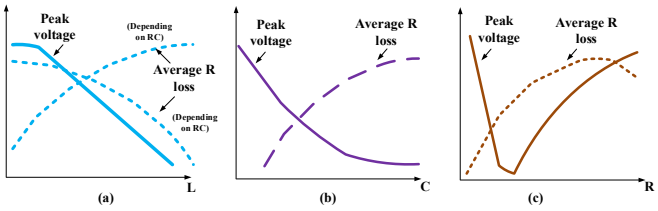


Fig. 9. L-C-R Parameter sweep and its impact on peak voltage and filter loss.

B. *Physical Design*

To achieve low power loss and reduce the efforts for inductor cooling, a high performance Co-based nanocomposite material developed by NASA Glenn Research Center (GRC) was applied in the dv/dt cores. These cores feature large and tunable magnetic anisotropy possible with tensile stress annealing and when optimized, also produce highly linear permeability with field strength compared to powder cores. In addition, the material demonstrates excellent thermal stability and low loss compared to best-in-class commercial material (MPP).

For high current applications, a single turn design is beneficial for thermal stress, mechanical design, and high frequency (HF) performance. Fig. 10 shows the good inductance linearity with H field of the fabricated toroidal-shaped gapless core for the single turn dv/dt inductor, measured in 1800 V pulse test. Here, the blue line shows an ideally linear permeability.

To capture the overall inductor current spectrum in a target application, the filter model is placed in the system level simulation model where dc source, motor controller, dv/dt filter, cable and motors are interconnected. Then to simplify the core loss estimation, the losses are decoupled among line frequency, switching frequency, and high frequency ranges [5-8]. Steinmetz parameters at each range can then be extracted from the dedicated high power permeameter, V/I measurements with power amplifier, or calorimetric measurements.

For inductors with small signal current such as low amplitude current test or current harmonics at the HF range for high power test, I^2R type measurement based on the real term μ'' of the complex permeability is also applicable. Fig. 11 illustrates the measured complex permeability of the GRC Co-rich gapless core vs the commercial off-the-shelf AMCC-32 gapped core, showing higher linearity and frequency. The μ" of GRC core is much smaller indicating lower core loss, which is also verified by the permeameter loss measurement from Fig. 12 that uses higher magnitude excitation fields near the expended dominant harmonic frequency.

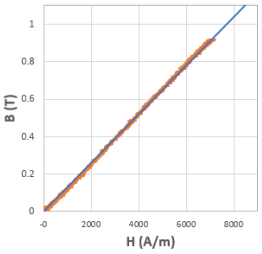


Fig. 10. Measured B-H curve of the fabricated GRC core.

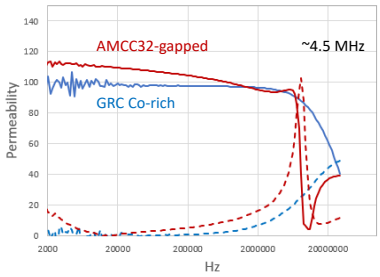


Fig. 11. Measured permeability of the GRC Co-rich gapless core vs the commercial off-the-shelf AMCC-32 gapped core.

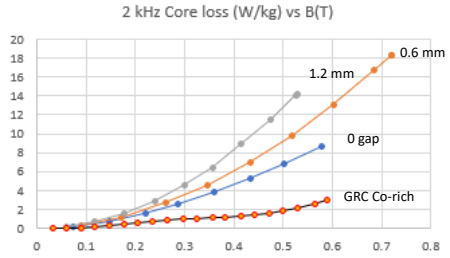


Fig. 12. Core loss measurement between GRC core and AMCC core using high power permeameter.

Fig. 13 shows the core loss estimated from the frequency spectrum measuredat the preliminary low phase current condition of the motor controller and the measured complex permeability. The majority of losses occur above 200 kHz due to harmonics but are indeed not significant through 500 Vdc. No temperature rise was measured in the cores following several minutes of operation that support this loss estimate.

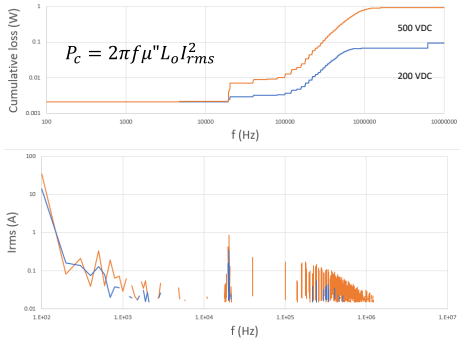


Fig. 13 Estimated core loss based on ac continuous excitation current spectrum and frequency dependent μ´´.

As for the RC components, Ohmite chassis mount resistors are used based on the required voltage rating and power rating. And HF film capacitors handling dv/dt type dynamics are adopted. Since the damping resistors in the LC-R filter topology suffer the highest power loss in this application condition, a cold plate has been selected to provide sufficient cooling.

IV. Experimental Verification

A. *Singe-phase Half-bridge Relfection Votlage Test*

Fig. 14 presents the protype of the GRC core based single-turn three-phase dv/dt filter. It is first tested in the test rig with single-phase half-bridge pulse tester and seven-meter cable. The load side is left with the open circuit to illustrate the worst

scenario. The three-phase shields are connected on both ends and grounded on the converter side. To mitigate the interface wire issue mentioned in Section II. B, the filter connection with the bulky cables and the motor controller terminals are improved to minimize the length of the interface wire as possible as we can. This improves the agreement between the simulation model and test reflection voltage compared to Fig 3 and Fig. 6.

Before adding the filter, the 750 V peak voltage overshoot and significant oscillations are observed on the cable far end and also occurs slightly on the converter side, as seen from Fig. 15 that compares the LTspice circuit model simulation and the measured test results.

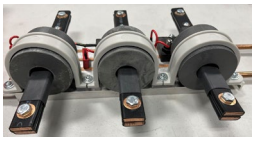


Fig. 14. Protype of the designed single-turn three-phase dv/dt filter.

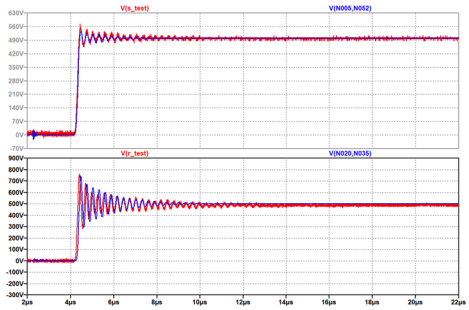


Fig. 15. Reflection voltage of modeling and testing results in the improved setup with shorter interface wire, and dv/dt filter is not applied. Top: converter side. Bottom: cable far-end side.

Fig. 16 shows the result after installing the filter. The reflection voltage on cable far-end is significantly reduced and the oscillations are quickly dampened. A good match again exists between the simulation model and test circuit. Figures 17 and 18 show detailed waveforms measured by two synchronized oscilloscopes on both ends of the 7-meter cables .

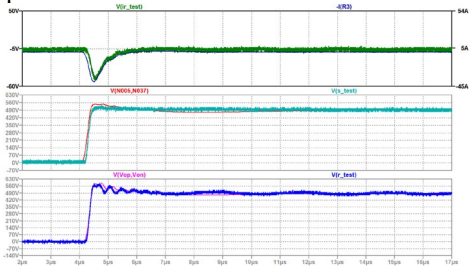


Fig. 16. Reflection voltage of modeling and testing results in the improved setup with shorter interface wire, and dv/dt filter is applied. Top: RC branch current. Middle: converter side voltage. Bottom: cable far-end side voltage.

Figure 19 shows detail of the reflection voltage on the cable far end with and without the filter to better illustrate the filter performance during the switching transient of the pulse voltage.

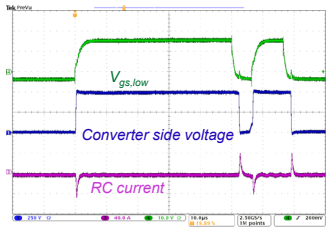


Fig. 17. Voltage and current at the converter side with the dv/dt filter.

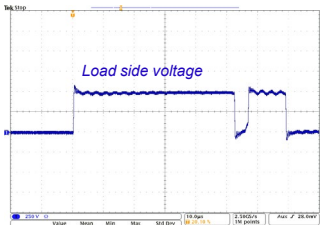


Fig. 18. Reflection voltage at the cable far end with the dv/dt filter.

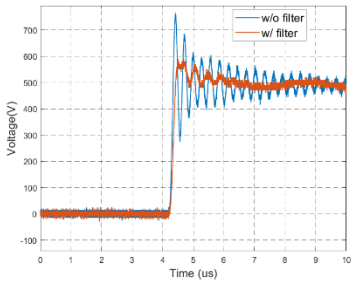
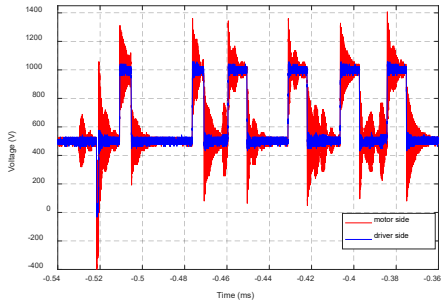


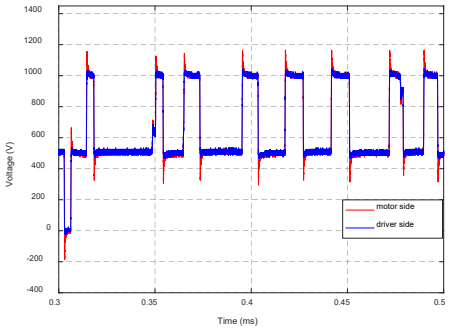
Fig. 19. Comparison of reflection voltage on the cable far end without and with the designed dv/dt filter.

B. Three-phase Relfection Votlage Test

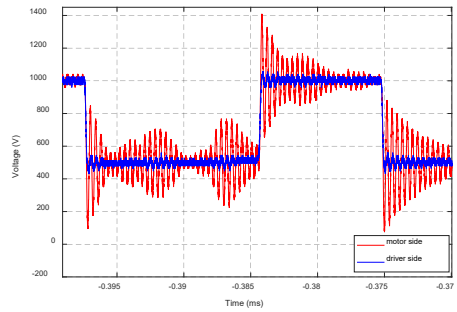
The three-phase dv/dt filter is also applied in a test rig with three-phase motor controller and seven-meter cable system. As observed in Fig 20, the designed filter effectively suppresses the voltage stress on the load side, and also eliminates most of the high frequency ringing harmonics, which is very helpful for reduction of HF motor loss and bearing current, and important for the mitigation of conducted and radiated EMI emission along the cable.



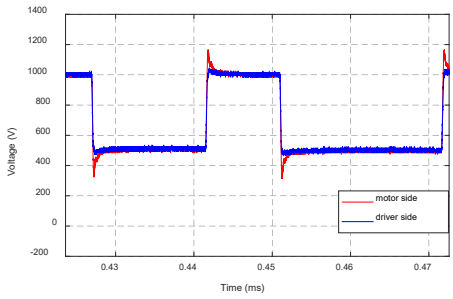
(a)



(b)



(c)



(d)

Fig. 20. Comparison of reflection voltages on cable far end (motor side) and converter side before and after adding the dv/dt filter. (a) before adding filter; (b) after adding filter; (c) zoomed-in of (a); (d) zoomed-in waveforms of (b).

CONCLUSION

In this paper, a comprehensive review of the state-of-art high frequency modeling approaches for transmission line effected related reflection voltage and oscillations in motor/generator systems is presented and discussed, and several new observation and challenges are discussed based on measurement, modeling, and testing comparison in this work. Particularly, aiming to the threats introduced by the high dv/dt speed of the popularized SiC PWM inverters nowadays, a practical modeling methodology of such driving systems and optimal design of the dv/dt filter are presented and experimentally verified, allowing the designer to quickly estimate the problem, select the proper components and implement the filter for low losses and compact design.

ACKNOWLEDGEMENT

The material is based upon work supported by the National Aeronautics and Space Administration under Contract Number NNC15BA05B.

REFERENCES

[1] R. J. Kerkman, D. Leggate and G. L. Skibinski, "Interaction of drive modulation and cable parameters on AC motor transients," IEEE Trans. Ind. Applicat., vol. 33, no. 3, pp. 722-731, May-June 1997.

[2] F. Wang and Z. Zhang, "Overview of silicon carbide technology: Device, converter, system, and application," CPSS Trans. on Power Electron. and Applicat, vol. 1, no. 1, pp. 13-32, Dec. 2016.

[3] L. Wang, C. Ngai-Man Ho, F. Canales and J. Jatskevich, "High-Frequency Modeling of the Long-Cable-Fed Induction Motor Drive System Using TLM Approach for Predicting Overvoltage Transients," IEEE Trans. Power Electron., vol. 25, no. 10, pp. 2653-2664, Oct. 2010.

[4] B. Narayanasamy, A. S. Sathyanarayanan, A. Deshpande and F. Luo, "Impact of cable and motor loads on wide bandgap device switching and reflected wave phenomenon in motor drives," IEEE Applied Power Electron. Conf. and Expo. (APEC), Tampa, FL, 2017, pp. 931-937.

[5] T. Shimizu and S. Iyasu, "A Practical Iron Loss Calculation for AC Filter Inductors Used in PWM Inverters," IEEE Trans. Ind. Electron., vol. 56, pp. 2600-2609, 2009.

[6] Q. Wang, X. Zhang, R. Burgos, D. Boroyevich, A. M. White and M. Kheraluwala, "Design and Implementation of a Two-Channel Interleaved Vienna-Type Rectifier With >99% Efficiency," IEEE Trans. Power Electron., vol. 33, no. 1, pp. 226-239, Jan. 2018.

[7] K. Venkatachalam, C. R. Sullivan, T. Abdallah and H. Tacca, "Accurate prediction of ferrite core loss with nonsinusoidal waveforms using only Steinmetz parameters," IEEE Workshop on Computers in Power Electronics, Proceedings., Mayaguez, Puerto Rico, USA, 2002.

[8] W. Shen, F. Wang, D. Boroyevich and C. W. Tipton IV, "High-Density Nanocrystalline Core Transformer for High-Power High-Frequency Resonant Converter," IEEE Trans. Ind. Applicat., vol. 44, no. 1, pp. 213-222, Jan.-feb. 2008.

[9] Micrometals Catalog CD-ROM, Micrometals Inc., Anaheim, CA, 2005.

[10] M. Bartoli, A. Reatti, and M. K. Kazimierczuk, “Minimum copper and core losses power inductor design,” in Conf. Rec. IEEE IAS Annu. Meeting, 1996, vol. 3, pp. 1369–1376.

[11] M. L. Heldwein, L. Dalessandro and J. W. Kolar, "The Three-Phase Common-Mode Inductor: Modeling and Design Issues," IEEE Trans. Ind. Electron., vol. 58, no. 8, pp. 3264-3274, Aug. 2011.

[12] S. Sundeep, J. Wang, A. Griffo and F. Alvarez-Gonzalez, "Antiresonance Phenomenon and Peak Voltage Stress Within PWM Inverter Fed Stator Winding," IEEE Trans. Ind. Electron., vol. 68, no. 12, pp. 11826-11836, Dec. 2021.

[13] S. Sundeep, J. Wang and A. Griffo, "Holistic Modeling of High-Frequency Behavior of Inverter-Fed Machine Winding, Considering Mutual Couplings in Time Domain," IEEE Trans. Ind. Applicat., vol. 57, no. 6, pp. 6044-6057, Nov.-Dec. 2021.

[14] L. Wang, Y. Zhang, M. S. Ali, G. Chen, J. M. Guerrero, and J. C. Vasquez, “High-Frequency Modeling and Filter Design for PWM Drives with Long Cables,” Energies, vol. 14, no. 4, p. 1155, Feb. 2021.

[15] MathWorks, PI Section Line. [Online]. Available: https://www.mathworks.com/help/sps/powersys/ref/pisectionline.html;jsessionid=ec7c9296a71bde700b78683951c9

[16] G. Skibinski, R. Tallam, R. Reese, B. Buchholz and R. Lukaszewski, "Common Mode and Differential Mode Analysis of Three Phase Cables for PWM AC Drives," Conf. Rec. IEEE Industry Applications Conference Forty-First IAS Annual Meeting, 2006, pp. 880-888.

[17] P. T. Caballero, E. C. M. Costa and S. Kurokawa, "Frequency-dependent line model in the time domain for simulation of fast and impulsive transients", Int. J. Electr. Power Energy Syst., vol. 80, Sep. 2016.

[18] C. Paul, Analysis of Multiconductor Transmission Lines, New York: Wiley, 2007.

[19] Y. Weens, N. Idir, R. Bausiere and J. J. Franchaud, "Modeling and simulation of unshielded and shielded energy cables in frequency and time domains," IEEE Trans. Magnet., vol. 42, no. 7, pp. 1876-1882, July 2006.

[20] P. C. Krause and K. Carlsen, “Analysis and hybrid computer simulation of multiconductor transmission systems,” IEEE Trans. Power App. Syst., vol. PAS-91, pp. 465–477, Mar./Apr. 1972.

[21] A. Sheri, A. De Beer, S. Padmanaban, A. Emleh and H. C. Ferreira, "Characterization of a power line cable for channel frequency response — Analysis and investigation," IEEE International Conference on Environment and Electrical Engineering and 2017 IEEE Industrial and Commercial Power Systems Europe (EEEIC / I&CPS Europe), 2017.

[22] Jason Jon Yoho, “Physically-Based Realizable Modeling and Network Synthesis of Subscriber Loops Utilized in DSL Technology”, Dissertation, Virginia Tech, 2001.

[23] E. Velander et al., "An Ultralow Loss Inductorless dv/dt Filter Concept for Medium-Power Voltage Source Motor Drive Converters With SiC Devices," IEEE Trans. Power Electron., vol. 33, no. 7, pp. 6072-6081, July 2018.